Molecular engineering of G-quadruplex ligands based on solvent effect of polyethylene glycol

Zi-Fu Wang[1,2] and Ta-Chau Chang[1,2,*]

[1]Department of Chemistry, National Taiwan University and [2]Institute of Atomic and Molecular Sciences, Academia Sinica, Taipei 106, Taiwan, R.O.C.

ABSTRACT

Because various non-parallel G-quadruplexes of human telomeric sequences in K^+ solution can be converted to a parallel G-quadruplex by adding polyethylene glycol (PEG) as a co-solvent, we have taken advantage of this property of PEG to study the covalent attachment of a PEG unit to a G-quadruplex ligand, 3,6-bis(1-methyl-4-vinylpyridinium) carbazole diiodide (BMVC). The hybrid ligand with the PEG unit, BMVC-8C3O or BMVC-6C2O by substituting either the tetraethylene glycol or the triethylene glycol terminated with a methyl-piperidinium cation in N-9 position of BMVC, not only induces structural change from different non-parallel G-quadruplexes to a parallel G-quadruplex but also increases the melting temperature of human telomeres in K^+ solution by more than $45°C$. In addition, our ligand work provides further confidence that the local water structure plays the key to induce conformational change of human telomere.

INTRODUCTION

Telomeres, the ends of chromosomes, are essential for the integrity of chromosomes by protecting them from degradation and end-to-end fusion (1–3). Telomeres contain guanine-rich DNA sequences. Of interest is that a short 3′-overhang with 100–200 bases of hexameric repeats of TTAGGG single-stranded sequence could adopt an intramolecular G-quadruplex (G4) structure under physiological conditions both *in vitro* (4,5) and *ex vivo* in the metaphase chromosome (6,7). Because the G4 structure is not a template of telomerase, the folding of telomeric DNA into G4 structures may inhibit telomerase activity (8,9). Such a structure might be a potential target for therapeutic cancer intervention (10–12). Small molecules that can induce G4 structure and further stabilize G4 structure have the potential to arrest tumor growth.

However, the G-rich sequence can adopt various G4 structures. For example, nuclear magnetic resonance (NMR) analysis showed that human telomeric sequence, $d[AG_3(T_2AG_3)_3]$ (A-HT21), forms a basket anti-parallel G4 structure (Scheme IA) in Na^+ solution (4), whereas X-ray crystallography showed that A-HT21 forms a propeller parallel G4 structure (Scheme IB) in the presence of K^+ (5). In addition, the co-existence of different G4 structures of A-HT21 in K^+ solution complicates the structural analysis (13–16). To complicate matters further, telomere sequences with slight differences can adopt other G4 structures, such as different hybrid forms of $d[TAG_3(T_2AG_3)_3]$ (TA-HT21) (Scheme IC) (13) and $d[TAG_3(T_2AG_3)_3TT]$ (TA-HT21-TT) (Scheme ID) (14) with three G-quartet layers versus a basket form of $d[G_3(T_2AG_3)_3T]$ (HT21-T) (Scheme IE) (17), with two G-quartet layers. Unfortunately, it is not known which of these structures are likely to be present in living cells so that the rational design of selective ligands to G4 is challenging.

It has been argued that the different G4 structures reported are because of different environmental conditions in which the structures have been determined. Miyoshi *et al.* (18–20) have used polyethylene glycol (PEG) to mimic cellular crowding environment and found that 2 M PEG can not only induce conformation change but also increase the stability of G4 structure. Chaires *et al.* (16) and Tan *et al.* (21) have showed that the crowding agent PEG induces dramatic changes in the G4 structure of human telomere in K^+ solution. Recently, Heddi and Phan (22) reported that the four different non-parallel G4 structures are all converted to a propeller G4 structure (Scheme I) under crowding PEG condition due to water depletion. This finding has reinforced the prevailing view that the parallel G4 structure is the form present in living cells. However, Trent *et al.* (23) have used 50% v/v acetonitrile as a dehydrating agent, and Dotsch *et al.* (24) have used either cell extract or Ficoll70 as a crowding solvent; these results have suggested that the parallel G4 structure of human telomeres formed under PEG conditions is not because of the crowding effect. Accordingly, the parallel G4 structure formed under PEG might not be physiologically prevalent

A (basket)   **B** (propeller)   **C** (mixed-I)   **D** (mixed-II)   **E** (basket)
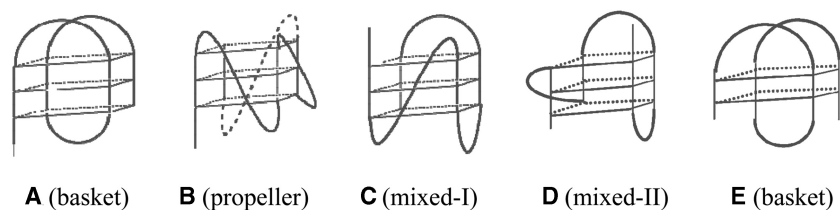
Scheme I.

(24). The question is whether concentrated PEG solutions mimic the condition of molecular crowding in cells, or whether the PEG-induced structural change arises from other effects.

It is well known that water molecules play an important role in DNA structure. At high concentrations, PEG is expected to disrupt the water structure. Is it possible that change in the water structure surrounding the DNA is promoting the shift in the equilibrium of the G4 structures toward the parallel form? If so, covalent attachment of a PEG unit to an existing G4 ligand may generate a hybrid ligand with similar properties. To test this hypothesis, a PEG unit, for example, tetraethylene glycol (TEG), with a methyl-piperidinium cation, is covalently attached to the G4 ligand 3,6-bis(1-methyl-4-vinylpyridinium) carbazole diiodide (BMVC), to generate the hybrid ligand, BMVC-8C3O. Indeed, the design principle based on PEG effect that can induce structural change and further stabilize the G4 structure provides a basis for the design of novel G4 ligands.

MATERIALS AND METHODS

Sample preparation

The syntheses of 9-substituted BMVC derivatives were shown in Scheme II. Briefly, compound **2a** was synthesized from 3,6-dibromocarbazole **1** (2 g, 6.15 mmole, Aldrich) through 9-position substitution by sodium hydride (0.295 g, 12.3 mmole, Aldrich) in Tetrahydrofuran (THF) (20 ml) under nitrogen. A dibromo alkane represented by the formula Br-R-Br (R = -CCOCCOCCOCC-) (100 mmole) was then added, and the mixture was refluxed for 12 hours. After cooling and quenching the waste sodium hydride with methanol, the solution was extracted with H_2O/ethyl acetate (1/1, v/v) twice, and the organic layer was dried by $MgSO_4$. The product **2a** was collected via flash column chromatography by a silica gel column with hexane/ethyl acetate (2/1, v/v) as the eluent.

The dry powder of compound **2a**, piperidine (0.5 ml, Aldrich) and NaH (1.5 mmole) was refluxed in DMF (20 ml) for 6 hours to obtain the compound **3a**, which was terminated by piperidine. The solvent was evaporated in vacuum, and the residue was purified via flash column chromatography by a silica gel column with hexane/ethyl acetate (1/2, v/v) as the eluent to collect the yellow product **3a**.

Then the product **3a** could couple with 4-vinylpyridine at mixed powders of Palladium (II) acetate/tri-o-tolylphosphine, under the triethylamine/acetonitrile solvent pairs in high-pressure system. After keeping the system under ∼105°C for 2 days, the precipitant was collected and then extracted with H_2O/CH_2Cl_2 (1:1, v/v) twice. The insoluble solids in CH_2Cl_2 layer were filtered and collected, washed with hot THF twice and then dried by $MgSO_4$. The crude powders were purified by flash column chromatography with acetone/n-hexane (1:1, v/v) as eluent to obtain the powders **4a**. The orange-red powders (BMVC-8C3O) were collected in good yield after refluxing the compound **4a** with excess CH_3I in acetone. The yield and NMR information are listed later:

NMR data

BMVC-8C3O

(Yield: 86%, mp > 300°C), ^{1}H NMR (400 MHz, DMSO-d6) δ: 8.80 (d, J = 6 Hz, 4H), 8.68 (s, 2H), 8.23 (d, J = 16 Hz, 2H), 8.20 (d, J = 7.2 Hz, 4H), 7.90 (d, J = 8.8 Hz, 2H), 7.76 (d, J = 8.4 Hz, 2H), 7.59 (d, J = 16 Hz, 2H), 4.64 (t, 2H), 4.24 (s, 6H), 3.82 (t, 2H), 3.71 (t, 2H), 3.47 (m, 4H), 3.38 (m, 10H), 2.97 (s, 3H), 1.67 (m, 4H), 1.43 (m, 2H).
^{13}C NMR (400 MHz, DMSO-d6) δ: 153.32, 145.24, 142.68, 142.28, 127.63, 127.21, 123.37, 123.14, 121.58, 121.04, 111.47, 70.48, 70.05, 69.87, 69.83, 63.87, 61.24, 47.21, 20.88, 19.71.

BMVC-6C2O

(Yield: 83%, mp > 300°C), ^{1}H NMR (400 MHz, DMSO-d6) δ: 8.81 (d, J = 6 Hz, 4H), 8.68 (s, 2H), 8.23 (d, J = 16 Hz, 2H), 8.21 (d, J = 7.2 Hz, 4H), 7.92 (d, J = 8.8 Hz, 2H), 7.76 (d, J = 8.4 Hz, 2H), 7.58 (d, J = 16 Hz, 2H), 4.68 (t, 2H), 4.33 (s, 6H), 3.85 (t, 2H), 3.68 (t, 2H), 3.51 (m, 2H), 3.42 (m, 6H), 2.99 (s, 3H), 1.67 (m, 4H), 1.43 (m, 2H).
^{13}C NMR (400 MHz, DMSO-d6) δ: 153.32, 145.30, 142.45, 142.38, 127.58, 127.21, 123.52, 123.32, 122.44, 121.68, 111.47, 70.38, 70.25, 69.97, 69.88, 63.92, 61.35, 48.20, 20.71, 19.66.

BMVC-8C

(Yield: 90%, mp > 300°C), ^{1}H NMR (400 MHz, DMSO-d6) δ: 8.82 (d, J = 6.4 Hz, 4H), 8.63 (s, 2H), 8.20 (d, J = 6.4 Hz, 4H), 8.19 (d, J = 16 Hz, 2H), 7.92 (d, J = 8.4 Hz, 2H), 7.77 (d, J = 8.4 Hz, 2H), 7.55 (d, J = 16 Hz, 2H) 4.48 (t, 2H), 4.24 (s, 6H), 3.25 (m, 6H), 2.94 (s, 3H),1.80
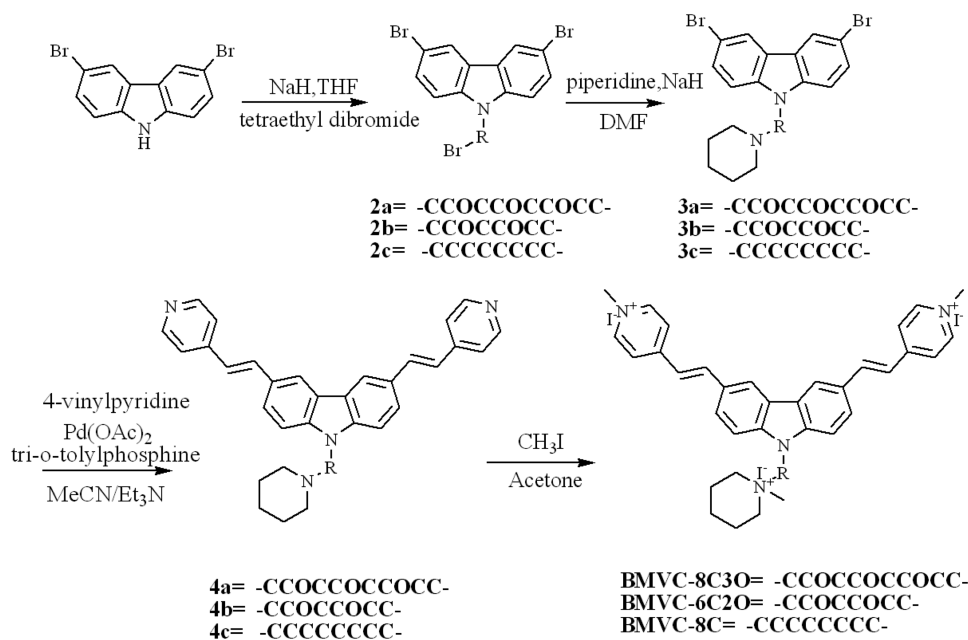
Scheme II.

(m, 2H), 1.73 (m, 4H), 1.59 (m, 2H), 1.50 (m, 2H), 1.30 (m, 4H), 1.24 (m, 4H).

^{13}C NMR (400 MHz, DMSO-d6) δ : 153.29, 145.26, 142.35, 142.28, 127.53, 127.30, 123.34, 123.07, 121.66, 121.02, 111.12, 60.32, 47.18, 28.98, 28.84, 26.75, 26.16, 21.27, 21.07, 19.66.

Chemical and sample preparation

All oligonucleotides were purchased from Bio Basic Inc. and used without further purification. Solutions of 10 mM Tris-HCl (pH 7.5) and 150 mM KCl mixed with each DNA were heated to 95°C for 10 min, cooled slowly to room temperature and then stored overnight at 4°C before use.

Circular dichroism

The circular dichroism (CD) spectra were averaged 10 scans on a J-815 spectropolarimeter (Jasco, Japan), with a 2 nm bandwidth at a 50 nm/min scan speed, and a 0.2 nm step resolution. The CD spectra were measured under N_2 over the range of 210–350 nm to ascertain the G4 structures.

Polyacrylamide gel electrophoresis (PAGE)

The PAGE was conducted using 20% polyacrylamide gels. Electrophoresis of the gels was carried out at 250 V/cm for 4 hours at 4°C. They were then photographed under ultraviolet (UV) light at 254 nm using a digital camera.

Imino proton NMR

Experiments were performed using 800 MHz Bruker spectrometers at 25°C. 1D NMR spectra were measured in H_2O/D_2O (90%/10%), using a jump and return sequence for solvent suppression. Strand concentration was 0.1 mM; the solution contained 10 mM Tris-HCl (PH 7.5) and 150 mM KCl, internal with reference Sodium 4,4-Dimethyl-4-silapentane-1-sulfonate (DSS).

Differential scanning calorimetry (DSC)

DSC thermograms were measured using an N-DSC III calorimeter (New Castle, DE). The data acquisition and analysis were carried out through the built-in software (NanoDSC Run version 3.6 and NanoAnalyze version 2.0). Each calorimetric experiment of 200 μM was performed by scanning from the sample from 20°C to 120°C at 1.0°C/min at 3 atm. This 3 atm prevents formation of gas bubbles and boiling of aqueous solutions above 100°C (25,26). The corresponding baseline (buffer-buffer) scans were subtracted from the buffer-sample scans before their normalization and analysis.

Analytical ultracentrifugation

Sedimentation experiments were performed using a Beckman Optima XLA analytical ultracentrifuge. Sedimentation velocity experiments of 0.5 OD DNA at 260 nm were conducted at 20°C using a rotor speed of 60 000 rpm. Data analysis was carried out with the program Sedfit (16,27).

RESULTS

Spectral change induced by BMVC-8C3O

CD has been applied to examine whether BMVC-8C3O can induce the spectral changes from the non-parallel to the parallel G4 structures of HT24 in K^+ solution. The

CD has been widely used to distinguish parallel from non-parallel G4 structures (28–33) because quartet stacking and strand orientation are the determining factors for the CD spectra. The positive CD band at 295 nm is characteristic of non-parallel G4 structure. Under PEG, the 295 nm band is notably diminished, and a strong positive band is detected at 265 nm, which is attributed to the formation of a parallel G4 structure. Figure 1a shows CD spectra of 20 µM HT24 in 150 mM K$^+$ solution after adding 1, 2, 3 and 5 eq. BMVC-8C3O for 2 h at 25°C (solid line), and their complexes after annealing (dash line). The annealing was performed by heating the solution to 95°C for 10 min and cooling slowly at 1°C/min to room temperature, followed by storage overnight. The CD spectra show no discernible difference before annealing, but appreciable change after annealing as a function of BMVC-8C3O concentration. The spectral conversion from the non-parallel pattern to the parallel pattern suggests that structural change of HT24 induced by BMVC-8C3O can be achieved by thermal activation.

To mimic physiological condition, we have examined whether BMVC-8C3O can induce structural change at 37°C. Figure 1b shows the CD spectra of 20 µM HT24 in 150 mM K$^+$ solution and its complex with 5 eq. BMVC-8C3O as a function of time at 37°C, as well as after annealing. After addition of BMVC-8C3O, the CD spectra show the decrease of the 295 nm band, together with the increase of the 265 nm band, as a function of time. Eventually, the time-evolved CD spectra more resemble the thermal-annealed spectrum. To confirm this, Figure 1c shows the high-resolution imino proton spectra of 100 µM HT24 in 150 mM K$^+$ solution and 2, 4, 6 and 12 h after addition of 5 eq. BMVC-8C3O at 37°C, as well as after annealing. After addition of BMVC-8C3O, the time-evolved NMR spectra show a rapid change followed by gradual change to the thermal-annealed spectrum. The rapid change may be because of interference of BMVC-8C3O, and the gradual change is likely because of structural change induced by BMVC-8C3O, consistent with the CD results. The time-evolved and thermal-activated NMR spectra suggest that the induced structures of HT24 by BMVC-8C3O are eventually the same. It appears that BMVC-8C3O can convert the non-parallel form to the parallel form of HT24 at moderate rates under physiological condition at 37°C.

The structural conversion induced by BMVC-8C3O was further confirmed by gel assay. The gel assays of HT24 in 150 mM K$^+$ solution on addition of 5 eq. BMVC-8C3O for overnight at 25°C and 37°C, as well as after annealing are shown in Figure 1d. These assays show two components with different migrations. The faster migration (lower) is the major component at 25°C, and the slower migration (upper) is the main component at 37°C. Tan *et al.* (21) have reported the structural conversion of HT21 induced by using 40% (v/v) PEG 200 and assigned the faster migration in the gel assays to the anti-parallel G4 structure and the slower migration to the parallel G4 structure. Evidently, temperature plays a critical role for structural conversion of HT24 induced by BMVC-8C3O.

Structural conversion from different non-parallel types to a parallel type induced by BMVC-8C3O

We have also examined whether BMVC-8C3O can convert different non-parallel G4 structures of human telomeres to the parallel G4 structure. Figure 2 shows the CD and the imino proton spectra of TA-HT21, A-HT21, HT21, HT21-T and a mutant sequence d[AG$_3$(CTAG$_3$)$_3$] (22CTA) (34) in 150 mM K$^+$ solution and after addition of 5 eq. BMVC-8C3O followed by annealing. The imino proton spectra of TA-HT21, HT21-T, and 22CTA in K$^+$ solution are consistent with the spectra reported by Heddi and Phan (22). It is found that the NMR spectra of TA-HT21, A-HT21, and 22CTA induced by BMVC-8C3O are similar to each other, although they have different G4 structures in K$^+$ solution without the ligand. The NMR patterns of TA-HT21, A-HT21 and 22CTA are slightly different from the patterns of HT21-T and HT21, with an extra single peak at ~11.5 ppm. This difference may be because of the 5'-flanking group in the former sequences, but not in the latter sequences (22). In addition, the corresponding CD spectra induced by BMVC-8C3O are also similar with each other. They all show a 265 nm positive CD band and a 240 nm negative CD band, characteristic of a parallel G4 structure.

In addition, we have examined whether these parallel G4 structures induced by BMVC-8C3O are similar to those converted under PEG. Figure 3a compares the imino proton spectra of 100 µM TA-HT21 in 150 mM K$^+$ solution after addition of 5 eq. BMVC-8C3O followed by annealing and a control in the presence of PEG. The imino proton spectrum of TA-HT21 in K$^+$ solution containing PEG is similar to that previously reported by Heddi and Phan (22). Similar imino proton spectra are observed for TA-HT21 between the addition of BMVC-8C3O and the presence of PEG, except for the line broadening noted in the latter, indicating that BMVC-8C3O can induce structural conversion of TA-HT21 from a hybrid G4 form to a parallel G4 form. Similar results were also found for A-HT21, HT21, HT21-T and 22CTA, as shown in Supplementary Figure S1. Thus, BMVC-8C3O can induce structural conversion of human telomeric sequences from different types of non-parallel G4 structures to a parallel type G4 structure in K$^+$ solution.

The time course of the NMR spectral changes highlights the evolution of the kinetic-driven products, and the annealed spectrum corresponds to that of the equilibrium structure. Supplementary Figure S2 summarizes the time-evolved imino proton spectra of TA-HT21, HT21-T and 22CTA, on addition of 5 eq. BMVC-8C3O at 37°C. They all showed rapid spectral change on addition of BMVC-8C3O followed by gradual change to the thermal-annealed spectra, consistent with the previous results for HT24 (Figure 1c). The much faster conversion rate for 22CTA than for HT21-T induced by BMVC-8C3O deserves further study. Nevertheless, the final structure is the same as the thermally activated structure, indicating that the structural conversion induced by BMVC-8C3O is feasible under physiological conditions.
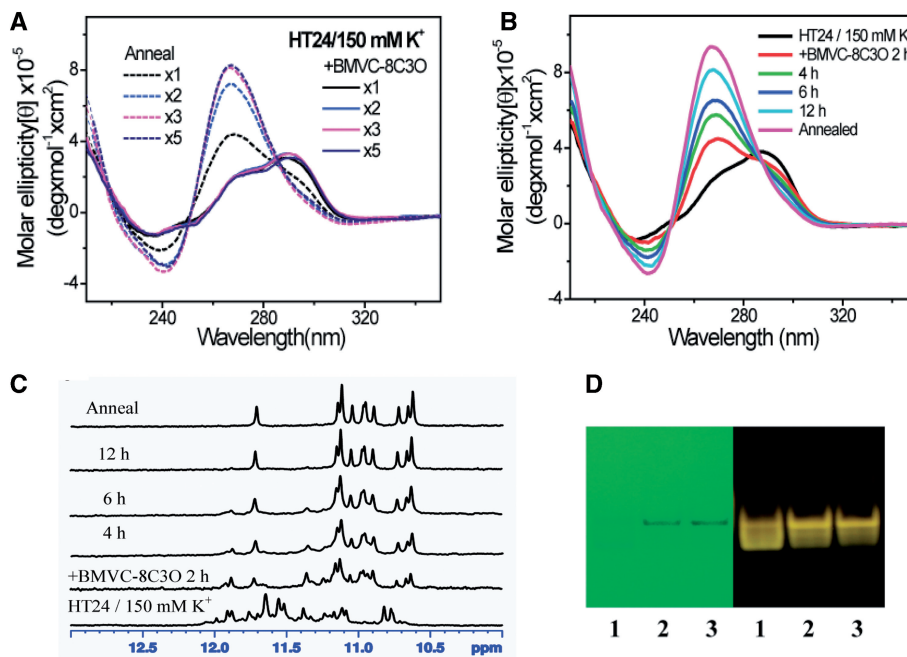
Figure 1. (**A**) CD spectra of 20 μM HT24 (solid line) and its complex with 1, 2, 3 and 5 eq. BMVC-8C3O (dash line) in 150 mM K$^+$ solution, as well as after annealing (dot). (**B**) Time-dependant CD spectra of 20 μM HT24 with 5 eq. BMVC-8C3O in 150 mM K$^+$ solution at 37°C. (**C**) High resolution imino proton spectra of 100 μM HT24 in 150 mM K$^+$ solution and 2, 4, 6 and 12 h after addition of 5 eq. BMVC-8C3O at 37°C, as well as after annealing. (**D**) UV shadowing and pre-stain of 0.2 nmol HT24 in 150 mM K$^+$ solution after adding 5 eq. BMVC-8C3O for overnight at 25°C (1) and 37°C (2), as well as after annealing (3).

Heddi and Phan (22) have further showed the conversion of the hybrid G4 structure to the parallel G4 structure can be reversed simply by quick dilution of the solution to a negligible PEG concentration. In contrast, the corresponding conformational transition of TA-HT21 induced by BMVC-8C3O is not reversible by sample dilution even overnight. Figure 3b shows the CD spectra of TA-HT21 induced by PEG and BMVC-8C3O followed by sample dilution. This difference is because of the global solvent effect versus the local ligand effect, which is important to discriminate the possible effects between molecular crowding and disruption of local water structure for conformational change.

### Melting temperature of G-quadruplex increased by BMVC-8C3O

We have further used DSC to measure the melting temperatures of TA-HT21 in 150 mM K$^+$ solution, on individual addition of 40% (v/v) TEG, 40% (v/v) PEG and 5 eq. BMVC-8C3O at 37°C overnight, as well as after annealing. These data are summarized in Figure 4a. The DSC shows a monophasic transition with the melting temperature (Tm) of ~70°C in 150 mM K$^+$ solution and ~97°C after addition of TEG (or PEG) overnight, a biphasic transition with the Tm of ~60°C and ~115°C after addition of BMVC-8C3O overnight at 37°C and a transition with the Tm of ~115°C with a shoulder at ~95°C after addition of BMVC-8C3O, followed by annealing. Similar results were also found in the DSC-melting curves of A-HT21, HT21-T, HT21 and 22CTA in 150 mM K$^+$ solution and on addition of 5 eq. BMVC-8C3O at 37°C overnight, as shown in Supplementary Figure S3.

In addition, Figure 4b shows the CD signals at 265 nm for TA-HT21 and its complexes after adding BMVC-8C3O for 12 h at 37°C in 150 mM K$^+$ solution. Here, the Tm of TA-HT21 measured from the CD melting curve is ~67°C, where the Tm of TA-HT21 measured from the DSC is ~70°C. Slight deviation of the Tm was also observed in the previous study of the bcl2mid under different K$^+$ concentration (35). Because the upper temperature of the CD melting curve is limited at 95°C, it indicates that the Tm of the TA-HT21/BMVC-8C3O complexes is much higher than 95°C.

Furthermore, the Tm of the G4 structure generally increases as a function of K$^+$ concentration (35–37). In accordance with this behaviour, DSC shows that the Tm of the major transition of TA-HT21 is ~45°C in 5 mM K$^+$ solution and ~97°C after addition of 5 eq. BMVC-8C3O at 37°C overnight, as shown in Figure 4c. Here, BMVC-8C3O also converts the G4 structure from the non-parallel form to the parallel form and increases the Tm of the G4 structure in 5 mM K$^+$ solution by more than 45°C.

Structural change of a longer telomeric sequence induced by BMVC-8C3O

The 3′-overhang single-stranded telomeric sequences are generally of 50–200 bases in length. We have examined the effects of BMVC-8C3O on the longer telomeric sequence d(T$_2$AG$_3$)$_8$ (HT48). Figure 5a shows the CD spectra of HT48 in 150 mM K$^+$ solution and after addition of 10 eq. BMVC-8C3O at 37°C for 2 and 12 h, as well as after annealing. In addition, Figure 5b shows the imino proton spectra of 100 μM HT48 in 150 mM K$^+$
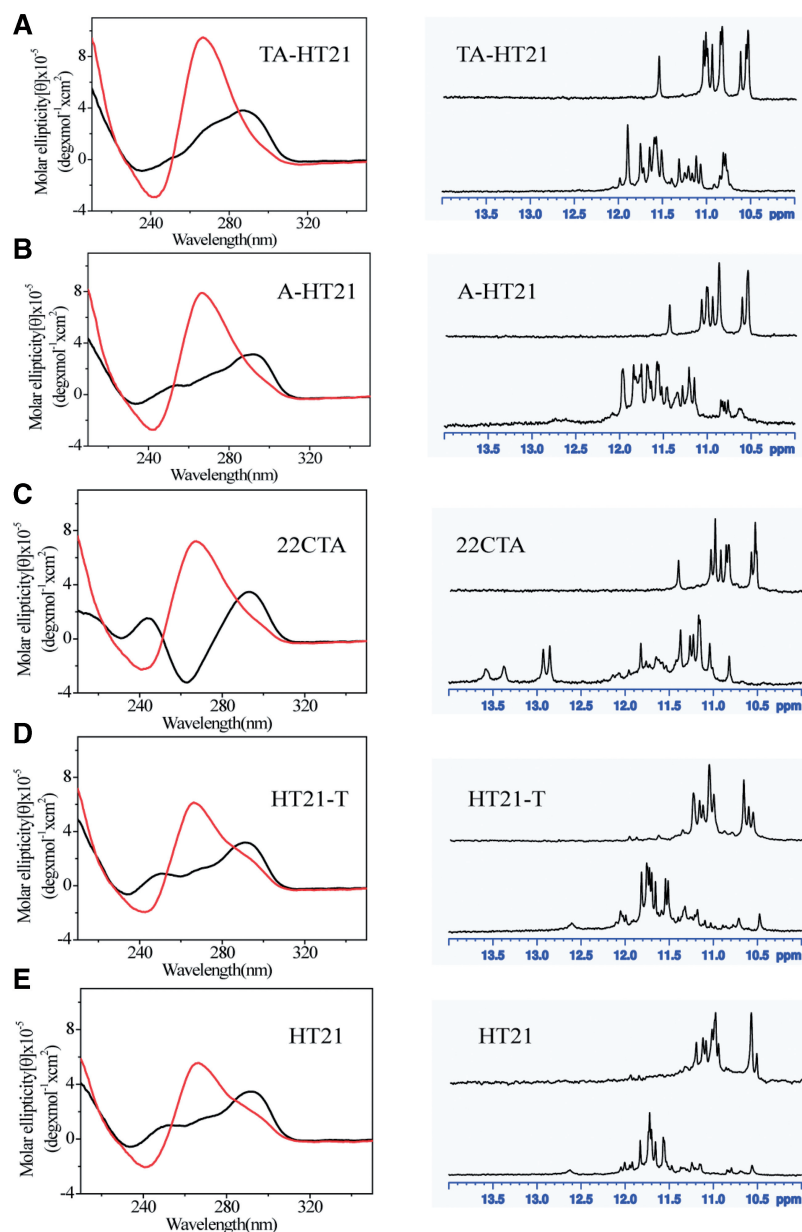
Figure 2. The CD spectra (left) of 20 μM (**A**) TA-H21, (**B**) A-H21, (**C**) 22CTA, (**D**) H21-T and (**E**) HT21 in 150 mM K^+ solution (black) and after addition of 5 eq. BMVC-8C3O followed by annealing (red). The imino proton NMR spectra (right) of 100 μM (**A**) TA-H21, (**B**) A-H21, (**C**) 22CTA, (**D**) H21-T and (**E**) HT21 and 22CTA in 150 mM K^+ solution (lower) and after addition of 5 eq. BMVC-8C3O followed by annealing (upper).

solution (lower), on adding 10 eq. BMVC-8C3O followed by annealing (upper), in the presence of PEG with (upper middle) and without (lower middle) addition of 10 eq. BMVC-8C3O. Figure 5c shows the DSC melting curves of HT48 in 150 mM K^+ solution and on addition of 10 eq. BMVC-8C3O at 37°C overnight. Although the precise structure of HT48 has not been determined yet, similar spectral change in CD and NMR patterns suggest that BMVC-8C3O can induce conformational change from a non–parallel-like G4 structure to a parallel-like G4 structure of HT48. Moreover, BMVC-8C3O can increase the Tm of HT48 in 150 mM in K^+ solution from ∼60°C to ∼120°C. It appears that BMVC-8C3O is a novel G4 stabilizer for a long telomere sequence as well.

## Structural change induced by BMVC-8C versus BMVC-6C2O

To test whether the oxygen in BMVC-8C3O plays an important role in the G4 structural conversion, we have further modified BMVC by substituting either an octane or a triethylene glycol in N-9 position with a methyl-piperidinium cation to give BMVC-8C or BMVC-6C2O, respectively. Figure 6a shows the CD spectra of TA-HT21 in 150 mM K^+ solution and its complex with 5 eq. BMVC-8C at 37°C for 12 h, as well as after annealing. We find that the structural conversion induced by BMVC-8C is much slower than that by BMVC-8C3O. In addition, NMR spectra show that the imino proton signals at ∼11.2, ∼11.3 and ∼11.9 ppm of
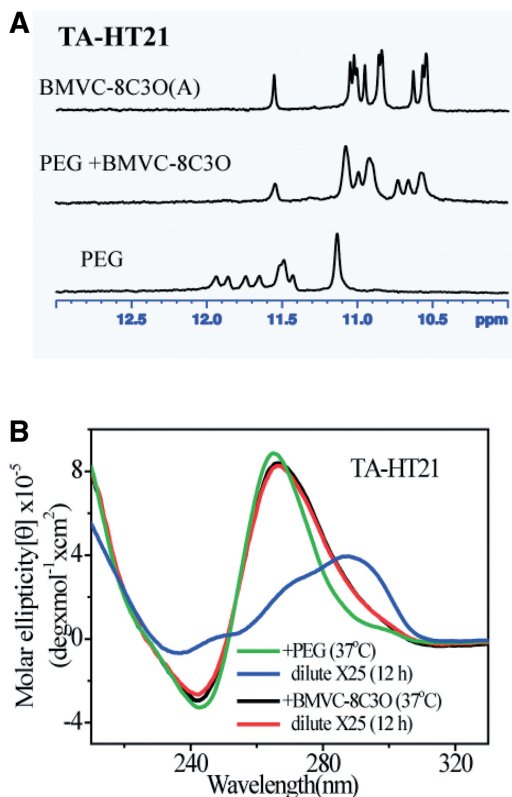
Figure 3. (**A**) The imino proton spectra of 100 μM TA-HT21 in 150 mM K$^+$ solution under 40% PEG condition (lower), followed by addition of 5 eq. BMVC-8C3O (middle) for 2 h, and TA-HT21 in 150 mM K$^+$ solution on addition of 5 eq. BMVC-8C3O followed by annealing (upper). (**B**) The CD spectra of TA-HT21 in 150 mM K$^+$ solution under 40% PEG and addition of 5 eq. BMVC-8C3O at 37°C and followed by sample dilution after 12 h at 37°C.

TA-HT21, after addition of BMVC-8C, disappeared in the annealed spectrum, are clearly detected after addition of BMVC-8C for 12 h in the time-evolved spectrum at 37°C (Figure 6b), supporting that the unfolding of the hybrid G4 structure of TA-HT21 by BMVC-8C at 37°C is slow. Of interest is that the imino proton spectra of TA-HT21 on addition of 5 eq. each BMVC-8C and BMVC-8C3O show some differences, implying different structural conversions induced by BMVC-8C and BMVC-8C3O. Figure 6c shows the gel assays of TA-HT21 in 150 mM K$^+$ solution on addition of 5 eq. BMVC-8 C for overnight at 25°C and 37°C, where the component with slow migration induced by BMVC-8C is even slower than that by BMVC-8C3O. We have further applied the sedimentation for ultracentrifugation analysis (16,27) to characterize monomer, dimer and higher order structures of TA-HT21. Figure 6d shows the sedimentation results of TA-HT21 on interaction with 5 eq. BMVC-8C after annealing. Our results show that BMVC-8C induces structural change of TA-HT21 from monomers to dimers together with some high order multimers.

We also studied the CD spectra, the imino proton spectra, the gel assays and the sedimentation analysis of TA-HT21 on addition of 5 eq. BMVC-6C2O, as shown in Supplementary Figure S4. Our results show that the
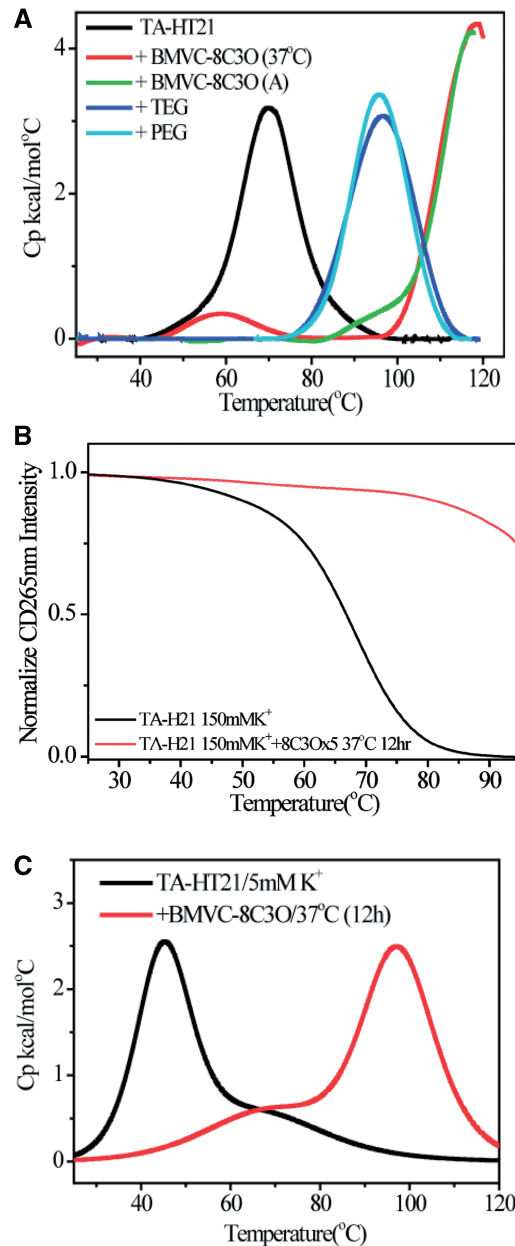
Figure 4. (**A**) The DSC of TA-HT21 in 150 mM K$^+$ solution (black), adding 40% TEG (blue), adding 40% PEG (light blue) and addition of 5 eq. BMVC-8C3O at 37°C overnight (red), as well as after annealing (green). (**B**) CD signals at 265 nm for the measurement of melting temperature of TA-HT21 (black) and its complexes of BMVC-8C3O (red) in 150 mM K+ solution as a function of temperature. (**C**) The DSC of TA-HT21 in 5 mM K$^+$ solution (black) and 12 h after addition of 5 eq. BMVC-8C3O (red) at 37°C.

oxygen in both BMVC-6C2O and BMVC-8C3O plays an important role in the structural transition of TA-HT21 from a monomer hybrid conformation to a monomer parallel conformation. It is not clear why different conformational changes are induced by BMVC-6C2O and BMVC-8C. The same non-parallel G4 structure converted to a monomer and a dimer of parallel G4 structures by these two hybrid ligands, is of interest and deserves further studies.
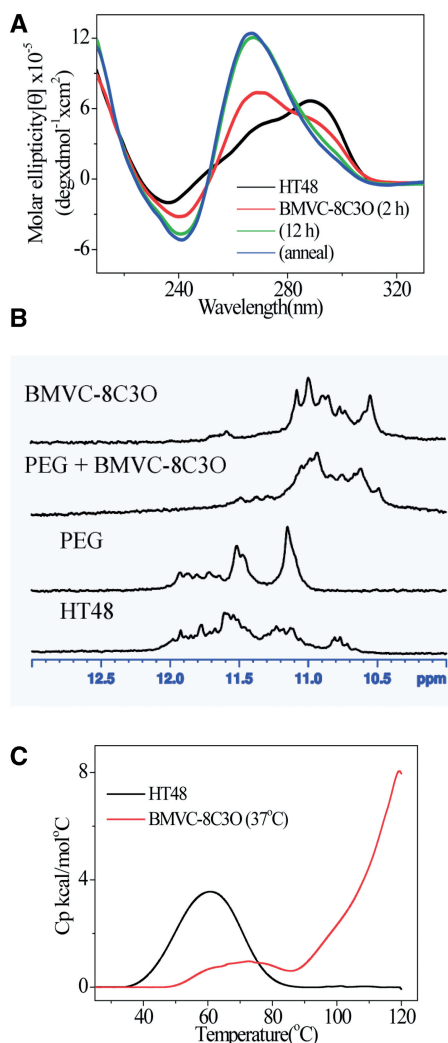
Figure 5. (**A**) Time-dependant CD spectra of 20 μM HT48 with 10 eq. BMVC-8C3O in 150 mM K⁺ solution at 37°C (**B**) The imino proton spectra of 100 μM HT48 in 150 mM K⁺ solution (bottom) under 40% PEG condition (lower middle) and 2 h after addition of 10 eq. BMVC-8C3O (upper middle) together with TA-HT21 in 150 mM K⁺ solution upon addition of 10 eq. BMVC-8C3O followed by annealing (upper). (**C**) The DSC of HT48 in 150 mM K⁺ solution (black) and addition of 10 eq BMVC-8C3O at 37°C (red) overnight.

DISCUSSION

Molecular crowding effect *vs.* local dehydration effect

In the past, the addition of 40% (v/v) PEG to the solutions has been used to mimic the condition of molecular crowding in cells. Although the PEG molecules are not expected to bind to the G4 structure specifically, at these high concentrations, they are sufficient to disrupt the water structure in the vicinity of the G4 structure. At the low concentration of several hundred μM BMVC-8C3O, there should be no global or gross disruption of the solvent structure by the PEG pendant. However, with the BMVC moiety bound to the G4 structure (29), the attached PEG is brought into the solvent sphere of the G4 structure. Only the water structure in the vicinity of the quadruplex-ligand complex is disrupted. In this manner, a reduced amount of the molecular surface

of the G4 structure is accessible to water. Water depletion favors the formation of the parallel form (22), as has been found in x-ray crystallography (5). Thus, we believe that the structural change induced by BMVC-8C3O is mainly because of a local dehydration effect. Consistent with this, no effects of sample dilution are expected because of the strong association of the BMVC-8C3O to the G4 structure (Figure 3b). Thus, our results provide further confidence that the local water structure plays the key to induce the various forms of the G4 structure to the parallel form.

Considering water molecules involved in DNA structure formation, Sugimoto *et al.* (38) suggested that hydration plays a major role for PEG in the stability of DNA, in contrast to viscosity and dielectric constant, which have little effects. In addition, the results reported by Trent *et al.* (23) using 50% (v/v) acetonitrile and Dotsch *et al.* (24), using Ficoll70 as a crowding solvent suggested that the structural change under PEG conditions is not because of the crowding effect. In this work, we have shown that the 100 μM BMVC-8C3O, which is not sufficient to generate a crowding environment, can successfully induce structural change of human telomeres to a parallel form. In contrast, the use of 100 μM BMVC is not able to induce various non-parallel G4 structures of human telomeres to the parallel G4 structure (29). Thus, it is the PEG unit in BMVC-8C3O that plays a major role in disrupting the local water structure in the vicinity of the G4 structure of human telomeres, and induces conformational change. With our hybrid BMVC-PEG ligand, we have discriminated between effects arising from molecular crowding and disruption of local water structure for conformational change. This is more than a subtle difference between our ligand work and earlier solvent studies.

Molecular engineering of G4 ligands

The first G4 binding ligand is an anthraquinone derivative reported by Sun *et al.* in 1997 (39). Since then, a growing number of G4 ligands, such as TMPyP4 (40), BRACO-19 (41), telomestatin (42), BMVC (43), naphthalene diimide (44) and pyridostatin (45) have been reported. Among them, the pyridostatin can increase the Tm of human telomere in 60 mM K⁺ solution up to 35°C (45). Most of the G4 ligands have common features, including a planar heteroaromatic core for the π–π interaction, with a terminal G-quartet and the presence of positive charge at side arms for the electrostatic interaction with sugar-phosphate backbone (46–48). However, none of them take into account the possible solvent effect from surrounding environment to further enhance the stability of folded structure. To our knowledge, this is the first report taking the advantage of the solvent effect to upgrade an existing G4 ligand that can disrupt the local water structure, which in turn can convert all multiple G4 structures of human telomeres to the parallel form and enhance the stability of G4-ligand structure significantly. Specifically, BMVC-8C3O can increase the Tm of d(T₂AG₃)₈ (HT48) from ∼60°C to ∼120°C in 150 mM K⁺ solution (Figure 5c) and that of TA-HT21 from ∼45°C to ∼97°C in 5 mM K⁺ solution (Figure 4b). This large increase in the melting temperature of human telomeres could possibly be
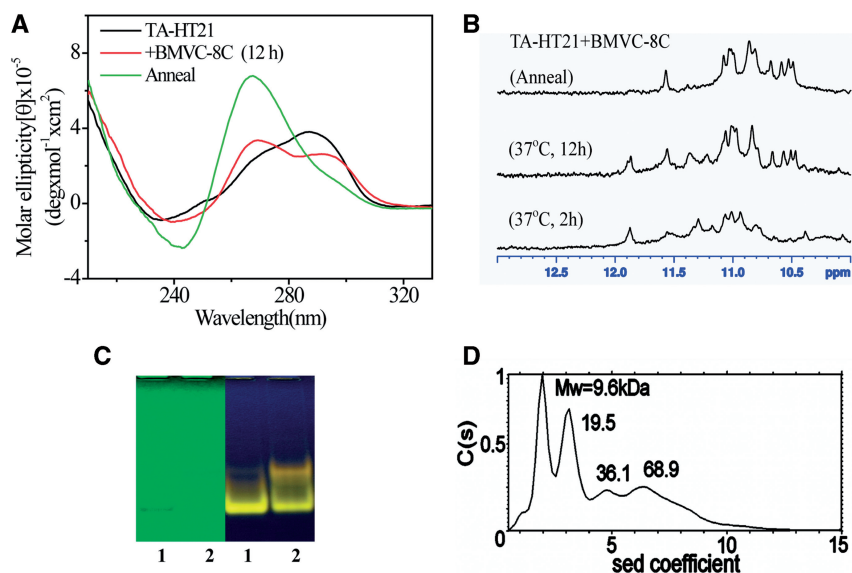
Figure 6. (**A**) Time-dependant CD spectra of 20 μM TA-HT21 with 5 eq. BMVC-8C in 150 mM K$^+$ solution at 37°C (**B**) Imino proton spectra of 100 μM TA-HT21 in 150 mM K$^+$ solution, 2 and 12 h after addition of 5 eq. BMVC-8C at 37°C, as well as after annealing. (**C**) UV shadowing and pre-stain of 0.2 nmol TA-HT21 in 150 mM K$^+$ solution after adding 5 eq. BMVC-8C for overnight at 25°C (1) and 37°C (2). (**D**) Ultracentrifugation of TA-HT21 in 150 mM K$^+$ solution on addition of 5 eq. BMVC-8C after annealing.

exploited for inhibiting telomerase activity. Biological studies and animal test of BMVC-8C3O are currently in progress.

Although the parallel G4 structure is unlikely the physioluable prevalent conformation, the important finding is that PEG can convert all non-parallel G4 forms to the parallel G4 form. To verify the possible mechanisms between molecular crowding and water depletion, we have taken advantage of this property of PEG to study the covalent attachment of a PEG unit to the G4 ligand, BMVC. Consistent with our hypothesis, the local water structure plays the key to induce conformational change of human telomere. Aside from this finding, the main thrust of our work is to outline a hybrid strategy with taking into account the solvent effect toward the development of an effective approach for drug design, and have provided a demonstration of "proof-of-principle".

SUPPLEMENTARY DATA

Supplementary Data are available at NAR Online: Supplementary Figures 1–4.

ACKNOWLEDGEMENTS

FUNDING

REFERENCES

1. Blackburn,E.H. (1984) The molecular structure of centromeres and telomeres. *Annu. Rev. Biochem.*, **53**, 163–194.
2. Williamson,J.R. (1994) G-quartet structures in telomeric DNA. *Annu. Rev. Biophys. Biomol. Struct.*, **23**, 703–730.
3. Cech,T.R. (2004) Beginning to understand the end of the chromosome. *Cell*, **116**, 273–279.
4. Wang,Y. and Patel,D.J. (1993) Solution structure of the human telomeric repeat d[AG$_3$(T$_2$AG$_3$)$_3$] G-tetraplex. *Structure*, **1**, 263–282.
5. Parkinson,G.N., Lee,M.P.H. and Neidle,S. (2002) Crystal structure of parallel quadruplexes from human telomeric DNA. *Nature*, **417**, 876–880.
6. Chang,C.C., Kuo,I.C., Ling,I.F., Chen,C.T., Chen,H.C., Lou,P.J., Lin,J.J. and Chang,T.C. (2004) Detection of quadruplex DNA structures in human telomeres by a fluorescent carbazole derivative. *Anal. Chem.*, **76**, 4490–4494.
7. Chang,C.C., Chu,J.F., Kao,F.J., Chiu,Y.C., Lou,P.J., Chen,H.C. and Chang,T.C. (2006) Verification of antiparallel G-quadruplex structure in human telomeres by using two-photon excitation fluorescence lifetime imaging microscopy of the 3,6-Bis(1-methyl-4-vinylpyridinium)carbazole diiodide molecule. *Anal. Chem.*, **78**, 2810–2815.
8. Bodnar,A.G., Ouellette,M., Frolkis,M. *et al.* (1998) Extension of life-span by introduction of telomerase into normal human cells. *Science*, **279**, 349–352.
9. Zahler,A.M., Williamson,J.R., Cech,T.R. and Prescott,D.M. (1991) Inhibition of telomerase by G-quartet DNA structures. *Nature*, **350**, 718–720.
10. Mergny,J.L. and Helene,C. (1998) G-quadruplex DNA: a target for drug design. *Nat. Med.*, **4**, 1366–1367.
11. Hurley,L.H. (2002) DNA and its associated processes as targets for cancer therapy. *Nat. Rev. Cancer*, **2**, 188–200.

12. Neidle,S. and Parkinson,G. (2002) Telomere maintenance as a target for anticancer drug discovery. *Nat. Rev. Drug Discov.*, **1**, 383–393.
13. Luu,K.N., Phan,A.T., Kuryavyi,V., Lacroix,L. and Patel,D.J. (2006) Structure of the human telomere in K^+ solution: an intramolecular $(3 + 1)$ G-quadruplex scaffold. *J. Am. Chem. Soc.*, **128**, 9963–9970.
14. Phan,A.T., Kuryavyi,V., Luu,K.N. and Patel,D.J. (2007) Structure of two intramolecular G-quadruplexes formed by natural human telomere sequences in K+ solution. *Nucleic Acids Res.*, **35**, 6517–6525.
15. Xu,Y., Noguchi,Y. and Sugiyama,H. (2006) The new models of the human telomere d[AGGG(TTAGGG)₃] in K^+ solution. *Bioorg. Med. Chem.*, **14**, 5584–5591.
16. Li,J., Correia,J.J., Wang,L., Trent,J.O. and Chaires,J.B. (2005) Not so crystal clear: the structure of the human telomere G-quadruplex in solution differs from that present in a crystal. *Nucleic Acids Res.*, **33**, 4649–4659.
17. Lim,K.W., Amrane,S., Bouaziz,S., Xu,W., Mu,Y., Patel,D.J., Luu,K.N. and Phan,A.T. (2009) Structure of the human telomere in K^+ solution: a stable basket-type G-quadruplex with only two G-tetrad layers. *J. Am. Chem. Soc.*, **131**, 4301–4309.
18. Miyoshi,D. and Sugimoto,N. (2008) Molecular crowding effects on structure and stability of DNA. *Biochimie*, **90**, 1040–1051.
19. Miyoshi,D., Karimata,H. and Sugimoto,N. (2006) Hydration regulates thermodynamics of G-quadruplex formation under molecular crowding conditions. *J. Am. Chem. Soc.*, **128**, 7957–7963.
20. Miyoshi,D., Matsumura,S., Nakano,S. and Sugimoto,N. (2004) Duplex dissociation of telomere DNAs induced by molecular crowding. *J. Am. Chem. Soc.*, **126**, 165–169.
21. Xue,Y., Kan,Z.Y., Wang,Q., Yao,Y., Liu,J., Hao,Y.H. and Tan,Z. (2007) Human telomeric DNA forms parallel-stranded intramolecular G-quadruplex in K^+ solution under molecular crowding condition. *J. Am. Chem. Soc.*, **129**, 11185–11191.
22. Heddi,B. and Phan,A.T. (2011) Structure of human telomeric DNA in crowded solution. *J. Am. Chem. Soc.*, **133**, 9824–9833.
23. Miller,M.C., Buscaglia,R., Chaires,J.B., Lane,A.N. and Trent,J.O. (2010) Hydration is a major determinant of the G-quadruplex stability and conformation of the human telomere 3′ sequence of d(AG₃(TTAG₃)₃). *J. Am. Chem. Soc.*, **132**, 17105–17107.
24. Hansel,R., Lohr,F., Foldynova-Trantirkova,S., Bamberg,E., Trantirek,L. and Dotsch,V. (2011) The parallel G-quadruplex structure of vertebrate telomeric repeat sequences is not the preferred folding topology under physiological conditions. *Nucleic Acids Res.*, **39**, 5768–5775.
25. Privalov,G., Kavina,V., Freire,E. and Privalov,P.L. (1995) Precise scanning calorimeter for studying thermal properties of biological macromolecules in dilute solution. *Anal. Biochem.*, **232**, 79–85.
26. Vetriani,C., Maeder,D.L., Tolliday,N. *et al.* (1998) Protein thermostability above 100°C: a key role for ionic interactions. *Proc. Natl. Acad. Sci.*, **95**, 12300–12305.
27. Stafford,W.F. and Sherwood,P.J. (2004) Analysis of heterologous interacting systems by sedimentation velocity: curve fitting algorithms for estimation of sedimentation coefficients, equilibrium and kinetic constants. *Biophys. Chem.*, **108**, 231–243.
28. Balagurumoorthy,P., Brahmachari,S.K., Mohanty,D., Bansal,M. and Sasisekharan,V. (1992) Hairpin and parallel quartet structures for telomeric sequences. *Nucleic Acids Res.*, **20**, 4061–4067.
29. Chang,C.C., Chien,C.W., Lin,Y.H., Kang,C.C. and Chang,T.C. (2007) Investigation of spectral conversion of d(TTAGGG)₄ and d(TTAGGG)₁₃ upon potassium titration by a G-quadruplex recognizer BMVC molecule. *Nucleic Acids Res.*, **35**, 2846–2860.
30. Bugaut,A. and Balasubramanian,S. (2008) A sequence-independent study of the influence of short loop lengths on the stability and topology of intramolecular DNA G-quadruplexes. *Biochemistry*, **47**, 689–697.
31. Masiero,S., Trotta,R., Pieraccini,S., De Tito,S., Perone,R., Randazzo,A. and Spada,G.P. (2010) A non-empirical chromophoric interpretation of CD spectra of DNA G-quadruplex structures. *Org. Biomol. Chem.*, **8**, 2683–2692.
32. Kypr,J., Kejnovska,I., Renciuk,D. and Vorlickova,M. (2009) Circular dichroism and conformational polymorphism of DNA. *Nucleic Acids Res.*, **37**, 1713–1725.
33. Gray,D.M., Wen,J.D., Gray,C.W., Repges,R., Repges,C., Raabe,G. and Fleischhauer,J. (2008) Measured and calculated CD spectra of G-quartets stacked with the same or opposite polarities. *Chirality*, **20**, 431–440.
34. Lim,K.W., Alberti,P., Guedin,A., Lacroix,L., Riou,J.F., Royle,N.J., Mergny,J.L. and Phan,A.T. (2009) Sequence variant (CTAGGG)ₙ in the human telomere favors a G-quadruplex structure containing a G.C.G.C tetrad. *Nucleic Acids Res.*, **37**, 6239–6248.
35. Lin,C.T., Tseng,T.Y., Wang,Z.F. and Chang,T.C. (2011) Structural conversion of intramolecular and intermolecular G-quadruplexes of bcl2mid: the effect of potassium concentration and ion exchange. *J. Phys. Chem. B*, **115**, 2360–2370.
36. Rachwal,P.A., Findlow,I.S., Werner,J.M., Brown,T. and Fox,K.R. (2007) Intramolecular DNA quadruplexes with different arrangements of short and long loops. *Nucleic Acids Res.*, **35**, 4214–4222.
37. Smargiasso,N., Rosu,F., Hsia,W., Colson,P., Baker,E.S., Bowers,M.T., De Pauw,E. and Gabelica,V. (2008) G-quadruplex DNA assemblies: loop length, cation identity, and multimer formation. *J. Am. Chem. Soc.*, **130**, 10208–10216.
38. Koumoto,K., Ochiai,H. and Sugimoto,N. (2008) Hydration is an important factor to regulate thermodynamic stability of a DNA duplex under molecular crowding conditions. *Chem. Lett.*, **37**, 864–865.
39. Sun,D., Thompson,B., Cathers,B.E., Salazar,M., Kerwin,S.M., Trent,J.O., Jenkins,T.C., Neidle,S. and Hurley,L.H. (1997) Inhibition of human telomerase by a G-quadruplex-interactive compound. *J. Med. Chem.*, **40**, 2113–2116.
40. Wheelhouse,R.T., Sun,D.K., Han,H.Y., Han,F.X.G. and Hurley,L.H. (1998) Cationic porphyrins as telomerase inhibitors: the interaction of tetra-(N-methyl- 4-pyridyl)porphine with quadruplex DNA. *J. Am. Chem. Soc.*, **120**, 3261–3262.
41. Read,M.A., Wood,A.A., Harrison,J.R., Gowan,S.M., Kelland,L.R., Dosanjh,H.S. and Neidle,S. (1999) Molecular modeling studies on G-quadruplex complexes of telomerase inhibitors: structure-activity relationships. *J. Med. Chem.*, **42**, 4538–4546.
42. Shin-ya,K., Wierzba,K., Matsuo,K., Ohtani,T., Yamada,Y., Furihata,K., Hayakawa,Y. and Seto,H. (2001) Telomestatin, a novel telomerase inhibitor from Streptomyces anulatus. *J. Am. Chem. Soc.*, **123**, 1262–1263.
43. Chang,C.C., Kuo,I.C., Lin,J.J., Lu,Y.C., Chen,C.T., Back,H.T., Lou,P.J. and Chang,T.C. (2004) A novel carbazole derivative, BMVC: a potential antitumor agent and fluorescence marker of cancer cells. *Chem. Biodivers.*, **1**, 1377–1384.
44. Parkinson,G.N., Cuenca,F. and Neidle,S. (2008) Topology conservation and loop flexibility in quadruplex-drug recognition: crystal structures of inter- and intramolecular telomeric DNA quadruplex-drug complexes. *J. Mol. Biol.*, **381**, 1145–1156.
45. Rodriguez,R., Muller,S., Yeoman,J.A., Trentesaux,C., Riou,J.F. and Balasubramanian,S. (2008) A novel small molecule that alters shelterin integrity and triggers a DNA-damage response at telomeres. *J. Am. Chem. Soc.*, **130**, 15758–15759.
46. De Cian,A., Lacroix,L., Douarre,C., Temime-Smaali,N., Trentesaux,C., Riou,J.F. and Mergny,J.L. (2008) Targeting telomeres and telomerase. *Biochimie*, **90**, 131–155.
47. Monchaud,D. and Teulade-Fichou,M.P. (2008) A hitchhiker's guide to G-quadruplex ligands. *Org. Biomol. Chem.*, **6**, 627–636.
48. Ou,T.M., Lu,Y.J., Tan,J.H., Huang,Z.S., Wong,K.Y. and Gu,L.Q. (2008) G-quadruplexes: targets in anticancer drug design. *Chem. Med. Chem.*, **3**, 690–713.